Contents lists available at GrowingScience

Engineering Solid Mechanics

homepage: www.GrowingScience.com/esm

The behavior of confined masonry walls against outside contact blast loading

Fatemeh Rahimi[a], Arash Bayat[a], Saeid Baranizadeh[b] and Peyman Beiranvand[a*]

[a]*Phd Candidate, Department of Civil Engineering, Razi University, Kermanshah, Iran*
[b]*Graduate student, Faculty of Civil Engineering and Transportation, University of Isfahan, Iran*

ARTICLEINFO

Article history:
Received 10 January, 2018
Accepted 29 May 2018
Available online
1 June 2018

Keywords:
Blast loading
Masonry wall
Contact
Damage
Numerical analyses

ABSTRACT

Study of behavior of building structures under blast loads is an important issue for design of high reliable structures made of concrete material. Hence, in previous studies the enclosed wall under blast loads, open-air explosion has been investigated through experiments. In this study, the experimental results reported in the literature for dynamic performance of a masonry wall subjected to high strain dynamic loads (i.e. contact blast and air burst test) are simulated numerically using finite element method (FEM) by utilizing soft particle hydrodynamics (SPH). Comparison of simulated numerical results with the experimental data demonstrates the ability and accuracy of FEM analyses in predicting the response of confined masonry walls subjected to dynamic loads.

1. Introduction

In recent decades, the increase of terrorism threats has led to more attention for structural dynamic response under explosion loading conditions. The structure response under explosion loads is a very complex problem that includes non-linear geometry and substance, time dependent structural deformation and loading rate dependent material properties. Traditional methods are involved with the single degree of freedom (SDOF) system analysis while this method is the preferable method for analysis and design of structures. However, SDOF method based on the simplified assumptions may not be adequate for reliable modeling of a structure with complicated geometry under complex loading conditions. Experimental investigation of this topic can provide intuitive observations and useful information about the explosion caused by the deformation and structural damage of the structure. A number of researchers have studied the dynamic behavior of building materials under explosive loads (Abou-Zeid et al., 2010; Alsayed et al., 2016; Barnett et al., 2010; Beiranvand et al., 2017). Schenker et al. (2005) performed the fracture tests on a full scale confined masonry wall that is either protected or unprotected. Time dependent measurements from the confined masonry wall response with high support adhesion coefficients to the explosion waves were registered successfully and the information obtained for verification and validation of the computer code were used. Urgessa and Maji (2009) performed an explosion test in full scale in a structure constructed by fiber reinforced polymers (FRP)

* Corresponding author.
E-mail addresses: Peyman51471366@gmail.com (P. Beiranvand)

doi: 10.5267/j.esm.2018.6.004

reinforced masonry wall. It was observed that reinforcement was capable to tolerate the explosion load. Smith et al. (1992) conducted a series of experiments by using tunnels with smooth walls and different geometries in 1:45 scale and rooms with designed small partial openings in which the results can be observed in small scales. Calibrated material and simulation based computer numerical model can be used as a powerful supplement for experimental analysis. Different numerical methods such as finite element method (FEM) and soft particle hydrodynamic (SPH) were developed and have been accepted widely for the analysis and design of structures. According to the wide researches performed by these methods, it can be derived that the despite the experimental method that always involves problems about safety, the computer methods which are based on numerical simulation can provide reasonable predictions for the structure response under dynamic loading.

Under explosion loading conditions, various modes of fracture including bending damage, shear damage and brick lamination damage can be observed in the structures. Bending damage is a desirable fracture mechanism because it leads to more flexibility and lets the structure to absorb the maximum energy. However, during the explosion tests on the confined masonry wall many researchers have found that over short loading duration, bending fracture can occur alone, providing that the shear capacity exceeds the bending capacity strength. By using reliable analysis method Wu et al. (2005) developed a unidirectional model that predicts the most probable fracture mechanism between bending and direct shear from a confined reinforced masonry wall. In addition to the bending and shear damage, the lamination of the confined masonry wall is another important mode of damage that often occurs in contact or near explosion. In such cases, explosion transfers large amount of energy in the form of stress wave propagation to the structure. Without structure deformation evidences, lamination damage, reduces the cross-sectional area and then element bearing capacity reduction occurs. Also the lamination of the confined masonry wall leads to the generation of many exploded parts with high speed that is a threat for the personnel and the equipment inside the structure. Ohtsu (1996) investigated experimentally and analytically the dynamic fracture of the confined masonry wall reinforced by FRP fibers and observed that the mean diameters and lamination fracture volume decreases significantly. Explosion waves and exploded parts impact is concentrated in one impact zone. The brick under this zone affect the members by the explosion waves and exploded parts impact in a depth of about two time of the maximum penetration depth. Abou-Zeid et al. (2011) by an experimental validation showed that generally panels reinforced by FRP have a better performance compared to the similar control panels without FRP reinforcement. Beiranvand et al. (2017) studied the effect of blast loading for concrete filled steel tube. In the present study, the modeling of contact explosion is performed in order to investigate the strength against the lamination damage of the confined masonry wall. The confined masonry wall with normal strength and confined masonry wall with high support adhesion coefficient were modeled under 1.2 Kg of contact charge. The lamination damage was calculated, discussed and investigated in both of these walls. In addition to the experimental investigation, numerical simulation was performed earlier for regenerating the contact explosion and free air explosion tests implemented. Numerical models were developed for both of the above two explosions and confined masonry wall. Finite element analysis was performed for free air explosion tests while the response of walls in their general response modes for example, bending and shear response modes was in elastic or plastic ranges. To simulate the contact explosion test, the finite element method is involved and the soft particle hydrodynamic method was used and SPH particles were used to simulate the above explosions and finite element was used for simulating the confined masonry wall. The results of the numerical simulations were compared to the results of the performed tests and the feasibility of the numerical methods was validated. Ghade (2018) studied the collapse structure reinforced concrete under blast loading.

2. Laboratory data

2.1 Properties of the tested specimens (Static strength)

The confined masonry wall studied in the present research was built by Alsayed et al. (2016) in the

laboratory. For numerical modeling, three dimensional nonlinear finite elements method was used in AUTODYN software. Table 1 shows properties of contact with mortar and also the cohesive properties and development fracture.

Table 1. Properties of correspondent contact with mortar

Shear strength in Z direction(MPa)	Shear strength in X direction (MPa)	Strength in Y direction (MPa)	Contact type
99.35	93.35	61	**Adhesion**
Friction coefficient =0.7	$\delta_m^{max} = 0.001$	$\alpha = 10$	**Fracture propagation**

2.2. Effect of strain rate and dynamic increase factor

It is commonly stated that under loading with high strain rate, the material properties are different compared to the static conditions. Strength increase can be presented by using the dynamic increase factor (DIF). For masonry wall with natural strength with a compressive strength ranging from 5 to 12 MPa, DIF factor can be calculated using the equations presented by (Malvar et al., 2007). For the compressive strength of mortar with natural strength, the DIF factor can be calculated using the following equation:

$$\mathrm{DIF} = \frac{f_c}{f_{cs}} = \begin{cases} \gamma_s \left(\frac{\varepsilon}{\varepsilon_s}\right)^{\frac{1}{3}} & \text{for } \varepsilon \geq 30 s^{-1} \\ \left(\frac{\varepsilon}{\varepsilon_s}\right)^{1.026x} & \text{for } \varepsilon \leq 30 s^{-1} \end{cases} \quad (1)$$

f_c: Dynamic compressive strength in ε

f_{cs}: Static compressive strength in ε_s

ε: Strain rate in range of 0.00003 to 300 s^{-1}

ε_s: Static strain rate at 0.00003

$$\log \gamma_s = 6.156\alpha - 2 \quad (2)$$

$$\alpha = \frac{1}{5+9\frac{f_{cs}}{f_{co}}}$$

$$f_{co} = 10 \text{ MPa}$$

For concrete tensile strength with natural strength, DIF factor can be calculated by the following equation:

$$\mathrm{DIF} = \frac{f_t}{f_{ts}} = \begin{cases} \beta \left(\frac{\varepsilon}{\varepsilon_s}\right)^{\frac{1}{3}} & \text{for } \varepsilon \geq 1 s^{-1} \\ \left(\frac{\varepsilon}{\varepsilon_s}\right)^{\delta} & \text{for } \varepsilon \leq 1 s^{-1} \end{cases} \quad (3)$$

The dynamic strength of the masonry wall has been rarely investigated till now. Walls with compressive strength up to 12 MPa were tested and it was found that the bearing capacity of the steel fibers reinforced wall is increased in dynamic tests due to the effects of the strain rate. Millard et al. (2010), performed the dynamic bending tensile test on concrete with extra high strength with different amounts of steel fibers. Results showed an increase in bending strength strain rate with the increase of fibers percentage. In fiber reinforced walls, fibers leads to resistance against the transvers propagation

of cracks by joining the intermediate area with lower strength. Thus, the effect of higher loading rate on the reduction of transverse cracks propagation is reduced. In the present study, there was no data for describing the wall material dynamic behavior and a DIF of 1 has been used in the wall simulation under explosion loads. This is a relatively conservative assumption. It is worth noting that most studies will be performed on the dynamic strength of the masonry materials by performing experimental SHPB tests and numerical simulations, with new DIF values.

3. Contact explosion test performance

In the investigated contact explosion tests, the masonry wall with dimensions equal to the specimen dimensions was tested. The confining effect of the provided steel frame is in the control of the support adhesion. 1.2 Kg detonation charge is placed into a cylinder with diameter to length ratio of 1 in front of the wall surface. Fig. 1 shows the installation procedure and steel protection equipment system for contact explosion test. Foundation steel plates were bolted and anchored to the base to maintain the stability of the test system and then the wall was placed on the steel equipment with simply support boundary. Table 2 presents the explosive weight and its distance from the wall that was considered in the analyses.

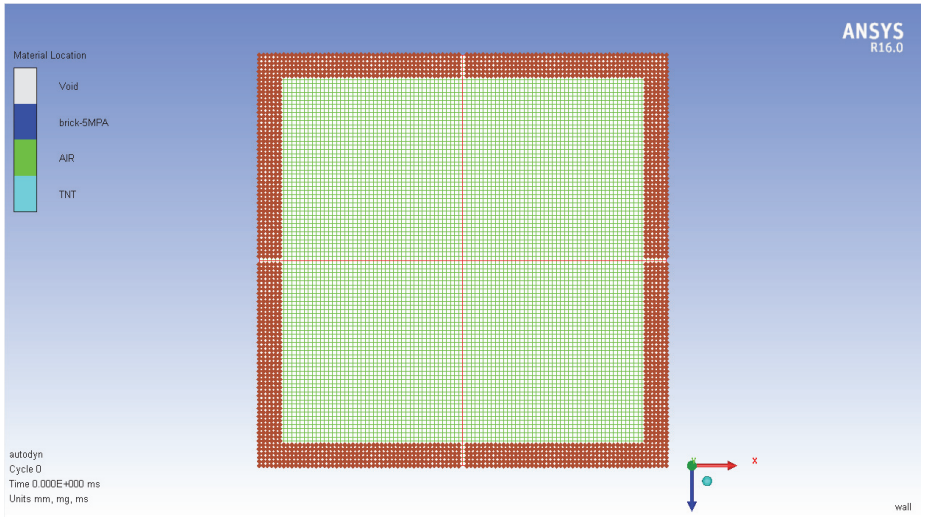

Fig. 1. Wall surrounding clamp conditions simulated in AUTODYN.

Table 2. Explosive weight and its distance from the wall

W(Kg)	$W_e(Kg)$	R(m)	$Z = R/\sqrt[3]{W_e}\ (m/Kg^{1/3})$	$t_a(ms)$	P(MPa)
1.134	1.55	4.8	4.14	7.87	0.146
49.9	68.4	4.8	1.17	2.72	0.772
14.2	19.4	2	0.74	0.755	2.065
113.4	155.4	4	0.74	1.496	2.098
500	685	4	0.45	1.027	5.236

Fig. 2 shows the response of the confined masonry wall after the 1.2 Kg contact explosion. It can be noted that the wall has experienced a fracture with a diameter of 390 mm on the adjacent (origin) surface, as is shown in Fig. 3. This is the lamination fracture mode and perforation of the conventional wall. Under contact loading conditions, the direct effects of the explosion pressure are applied on the adjacent surface and this pressure easily exceeds the dynamic compressive strength limit of the concrete and leads to the fracture initiation of concrete. Also the explosion load leads to strong stress wave propagation in the wall depth direction. The incident and reflective stresses interact, if the resulted final stresses exceed the bricks dynamic tensile strength limit that results in brick lamination. It is believed that such fracture occurs as a result of stress wave propagation inside the wall. Since the deviation of

the explosive starts from the center toward the surroundings, the waves of the incident stresses have a small distance to travel before the confronting of the reflective stress wave occurs from the free edge or boundary. Only a small amount of energy is dissipated before the wave coincidence and the final stress is still more than the brick dynamic tensile strength.

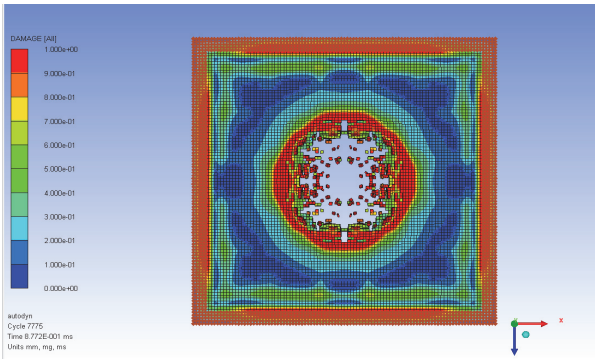

Fig. 2. Brick wall with clamp after contact explosion

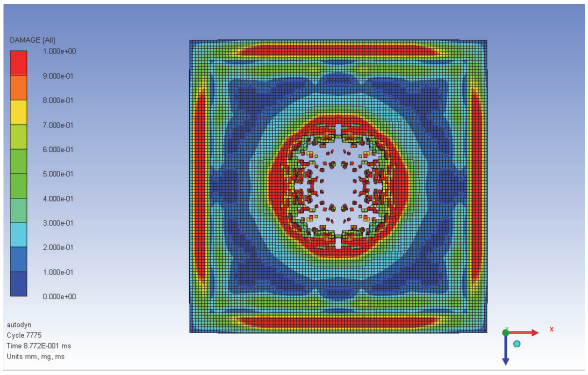

Fig. 3. Presentation of the clamp-free wall destruction after contact explosion

4. Numerical simulation of the brick wall under explosion in free air

In this section, the wall behavior is studied under various explosion loads and the proposed numerical model for the free-air explosion test performed by (Wu et al., 2011) and present contact explosion test is investigated numerically. Material properties, dimensions and test system in the free-air explosion experiments are the same with the contact explosion tests discussed above. Fig. 4 shows the model of wall under free-air explosion.

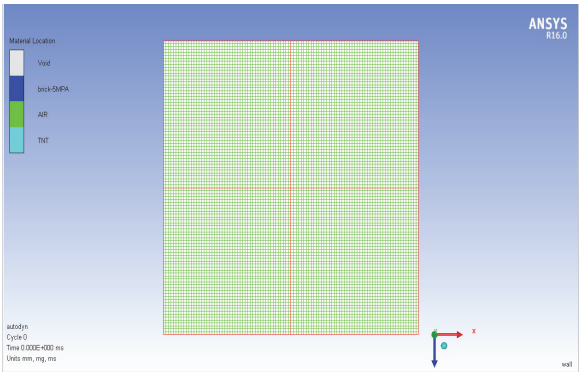

Fig. 4. Simulated model of the brick wall under free-air explosion.

4.1 Materials model

Numerical investigation in the present study has been performed by AUTODYN which is especially developed for the non-linear dynamic simulation. In AUTODYN, different material models such as pseudo-tensor (MAT_16), brittle damage (MAT_96), William & Wamke wall (MAT_11) and wall Rel3 damage (MAT_72_REL) can be used for the masonry wall simulation under dynamic loading conditions. William and Wamke is a model based on the plasticity and three shear fracture levels are used for which the deformation is dependent on the confinement pressure. Damage effect and strain rate are considered in this model. The main advantage of this model is that it is not confined based on a user input parameter, e.g. compressive strength. The remaining parameters of the model are created automatically using a built-in algorithm which can be modified by the user. In the previous sections, the appropriate materials model for the modeling of the simple brick brittle behavior was mentioned. But they cannot be a suitable model for the hardening damage behavior after the brick and mortar yield point. In addition, these models include many parameters which will be determined by a simple test on

the materials. In the present study, the materials properties are presented by the brick manufacturer and are limited to the stress-strain relation of the uniaxial compression and the stress-strain relation of the bending tension. For using many of the available experimental data, the hydrodynamic model of the materials, elastic-plastic hydrodynamic model, is used for describing the masonry wall dynamic behavior. This model can be simplified as a bilinear elastic-plastic stress-strain relation which is suitable for most of engineering materials including concrete for which the yield behavior is dependent on the pressure. Yield strength is a function of the effective plastic strain as:

$$\sigma_y = \sigma_0 + E_h \varepsilon^{-p}, \tag{4}$$

where σ_0 is the initial yield strength and E_h is the plastic hardening module defined in Young module parameters and E_t is the tangential module. For example:

$$E_h = \frac{EE_t}{E - E_t}. \tag{5}$$

Using the uniaxial compression test data, the relation between the effective stress and effective plastic strain can be determined. The interpolation of data curve cane be executed and in this case, E_h parameter is not required for the input during the calculations. Effective stress is defined as one of the parameters of the deviation stress tensor.

$$S_{ij} = \sigma_{ij} - \frac{1}{3}\sigma_{kk}\delta_{ij} \tag{6}$$

$$\overline{\sigma} = \sqrt{\frac{3}{2}S_{ij}S_{ij}} \tag{7}$$

The effective plastic strain can be defined as below:

$$\varepsilon^p = \int_0^t (\frac{2}{3}\varepsilon_{ij}^p \varepsilon_{ij}^p)^{\frac{1}{2}} dt, \tag{8}$$

In which *t* shows the time and ε_{ij}^p represents the plastic strain rate. The shock response was considered UHPC by using Mie-Gruneisen state equation. With particles shock velocity-particles velocity, Gruneisen state equation, defines the pressure for compressed materials as below:

$$P = \frac{\rho_0 C^2 \mu[1 + \left(1 - \frac{\gamma_0}{2}\right)\mu - \frac{a}{2}\mu^2]}{[1 - (S_{11} - 1)\mu - S_{22}\frac{\mu^2}{\mu+1} - S_{33}\frac{\mu^3}{(1+\mu)^2}]^2} + (\gamma_0 + a\mu)E \tag{9}$$

and for expanded material is:

$$P = \rho_0 C^2 \mu + (\gamma_0 + a\mu)E, \tag{10}$$

$$\mu = \frac{\rho}{\rho_0 - 1}, \tag{11}$$

in which C is the bulk sound velocity that is obtained from the U_S-U_p curve. S is the slope (deviation) coefficients of the U_S-U_p curve. The shock velocity-particles velocity is non-linear and is given as below:

$$U_s = C + S_{11}U_p + S_{22}\left(\frac{U_p}{U_s}\right)U_p + S_{33}(\frac{U_p}{U_s})^2 U_p. \tag{12}$$

It is formally well known that for most materials, second order and higher (term) conditions are negligible and thus parameters S_1 and S_3 will be set to zero thereafter. U_s shock velocity is a linear variable. According to the particles velocity, we have:

$$U_s = C + S_{11}U_p \,. \tag{13}$$

From macroscopic point of view, concrete is an isotropic material. For isotropic elastic members, the sound bulk velocity C is determined as below:

$$C = \sqrt{\frac{K}{\rho}}, \tag{14}$$

where K is UHPC bulk module that is equal to $\frac{2E}{9(1-2\gamma)}$. Consequently, in the present study, the nonlinear hardening behavior of the masonry wall stress was modeled by tabulating the stress-strain curve of the materials elastic-plastic hydrodynamic model in AUTODYN. Tensile stress fracture was determined by the tension cut-off value that was equal to 8 MPa according to the wall tensile stress. After substituting Young module, material density (1650 kg/m^3) and Poisson ratio (0.15) in Eq.12, then the bulk velocity is estimated to be 2100 m/s. According to the lack of dynamic test information, the slope of U_S-U_p curve, i.e. S_1 and Gruneisen gamma were obtained from the last numerical simulations for the steel fibers reinforced masonry wall. This model allows the definition of an arbitrary stress-strain curve and an arbitrary strain rate curve. However, fracture can defined based on a plastic strain or the minimum time step. Cracking and lamination in brick can be simulated by AUTODYN (using tied node with fracture definition and or element erosion algorithm). The first method needs defining repetitive nodes and their tying together at the selected zones. Using the erosion algorithm, the brick finite element model is created in the conventional method and when the element response (such as the principal stress or strain) exceeds the defined value, these elements are eliminated from the finite element method automatically.

4.2 Simulation of free-air explosion tests

Modeling of the explosion load in free-air explosion was performed by the load-explosion function in AUTODYN. This function avoids the accurate modeling of detonation charge and the propagation of shock wave in the air and can reduce the time required for the numerical analyses.

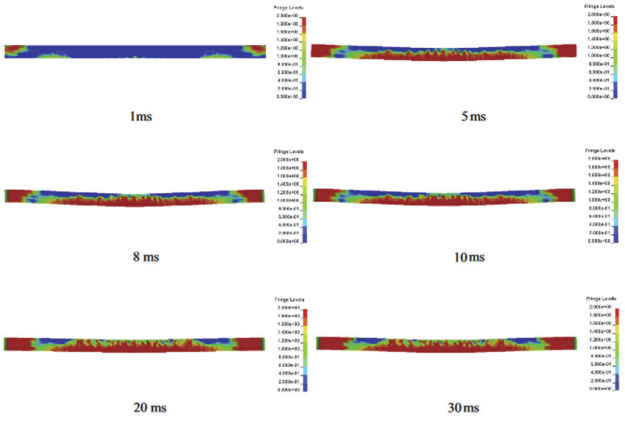

Fig. 5. Wall vertical face response with plastic strain contour

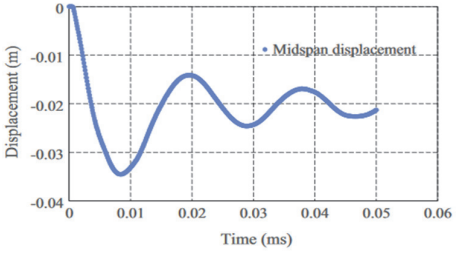

Fig. 6. Time history curve for mid-span deformation of wall

The disadvantage of this function is that it cannot model the shock waves and the structure interaction. In this section, free-air explosion is simulated on two confined masonry walls with different adhesion coefficients. Numerical results are then compared to the experimental results. Fig. 5 shows the wall vertical face response with the plastic strain contour. It can be observed that the wall deformation is in the plastic range and scrapping and laminations damage does not occur. These contours show that the concentration of cracks in the wall is mainly in the mid-span and the cracks

length is decreased by moving toward the wall boundary. In the experiments, LVDT was used for measurement of wall displacement after the first peak. Thus the comparison of the complete history curve is not available here. However, it should be noted that during the test, the peak displacement in the first vibration period was measured equal to 38mm (as shown in Fig. 6). This figure was in very good agreement with the results of numerical simulation that yields an amount of 36mm. a little underestimation in this regard can be due to the effect of detonation charge shape. The explosion used in this test has a cylinder container and despite this in AUTODYN, the load-explosion function was based on free-air spherical TNT explosion.

5. Conclusion and summary

The results of two dynamic blast tests on a confined masonry wall (contact and free-air explosion tests) were simulated numerically using finite element method. Free-air explosion and the current contact explosion tests are created in the AUTODYN hydro-code by the recommended numerical models. The finite element method is used for the simulation of free-air explosion, however, SPH and finite element methods are involved for the simulation of contact explosion. By comparing the results of damage mode and the exploded damaged observed in laminated zone it was concluded that the presented numerical model and the used methodology can provide a suitable response for the masonry wall loaded by dynamic and high strain rate loads.

References

Abou-Zeid, B. M., El-Dakhakhni, W. W., Razaqpur, A. G., & Foo, S. (2010). Response of arching unreinforced concrete masonry walls to blast loading. *Journal of Structural Engineering*, *137*(10), 1205-1214.

Alsayed, S. H., Elsanadedy, H. M., Al-Zaheri, Z. M., Al-Salloum, Y. A., & Abbas, H. (2016). Blast response of GFRP-strengthened infill masonry walls. *Construction and Building Materials*, *115*, 438-451.

Barnett, S. J., Lataste, J. F., Parry, T., Millard, S. G., & Soutsos, M. N. (2010). Assessment of fibre orientation in ultra high performance fibre reinforced concrete and its effect on flexural strength. *Materials and Structures*, *43*(7), 1009-1023.

Beiranvand, P., Omidinasab, F., Sadate Moayeri, M., Mehdipour, S., & Zarei, M. (2017). Finite Element Analysis for CFST Columns under Blast Loading. *Journal of Applied and Computational Mechanics*, *3*(4), 283-292.

Ghada, M.H. (2018).Collapse Analysis of a reinforced concrete frame due to middle column loss by explosion. *Journal of Civil Engineering and Structures, 2*(2), 10-24

Malvar, L. J., Crawford, J. E., & Morrill, K. B. (2007). Use of composites to resist blast. *Journal of Composites for Construction*, *11*(6), 601-610.

Ohtsu, M. (1996). The history and development of acoustic emission in concrete engineering. *Magazine of Concrete Research*, *48*(177), 321-330.

Schenker, A., Anteby, I., Nizri, E., Ostraich, B., Kivity, Y., Sadot, O., ... & Ben-Dor, G. (2005). Foam-protected reinforced concrete structures under impact: experimental and numerical studies. *Journal of structural Engineering*, *131*(8), 1233-1242.

Smith, P. D., Mays, G. C., Rose, T. A., Teo, K. G., & Roberts, B. J. (1992). Small scale models of complex geometry for blast overpressure assessment. *International Journal of Impact Engineering*, *12*(3), 345-360.

Urgessa, G. S., & Maji, A. K. (2009). Dynamic response of retrofitted masonry walls for blast loading. *Journal of Engineering Mechanics*, *136*(7), 858-864.

Wu, C., Hao, H., & Lu, Y. (2005). Dynamic response and damage analysis of masonry structures and masonry infilled RC frames to blast ground motion. *Engineering Structures*, *27*(3), 323-333.

Wu, K. C., Li, B., & Tsai, K. C. (2011). The effects of explosive mass ratio on residual compressive capacity of contact blast damaged composite columns. *Journal of Constructional Steel Research*, *67*(4), 602-612.